Electronic Supplementary Material (ESI) for Polymer Chemistry.

Supproting Information

Ring opening copolymerization of δ-valerolactone with 2-methyl-1,3-dioxane-4-one towards poly(3-hydroxypropionate-co-5-hydroxyvalerate) copolyesters

Wenli Zhang[#], Li Han[#], Zhipeng Liu, Yidi Li, Jingzhao Shang, Xuefei Leng*, Yang Li, Zhiyong Wei*

[a] Department of Polymer Science and Engineering, School of Chemical Engineering, Dalian University of Technology, Dalian 116024, P. R. China

*Corresponding author, E-mail address: lengxuefei@dlut.edu.cn (X. Leng), zywei@dlut.edu.cn (Z. Wei).

Experimental Section

Materials. All chemicals were used as received from Sigma-Aldrich unless otherwise specified. All air- and moisture-sensitive reactions were carried out using standard Schlenk-line techniques. All monomers were dried over CaH_2 at least 3h, fractionally distilled under vacuum and stored under a nitrogen atmosphere prior to use. All solvents we used were freshly distilled from sodium-benzophenone and sodium. The cyclic ester-acetal monomer 2-methyl-1,3-dioxan-4-one (MDO) was synthesized from commercial 2-methyltetrahydrofuran-3-one, as has recently been reported. Diethyl zinc catalyst (1.0 M in Toluene) were stored under a dry nitrogen atmosphere prior to used.

Methods.

Nuclear Magnetic Resonance (NMR) Spectrometer. $^{1}H/^{13}C$ NMR spectra were recorded on Avance (Bruker Co., Ltd., Germany) 400, 500, and 600 MHz spectrometers (TMS, δ=0ppm, as the internal standard).

Gel permeation chromatography (GPC). The number-average molecular weight (M_n), weight-average molecular weight (M_w), and the polydispersity index (PDI) were determined by a Waters 1515 GPC (USA) gel permeation chromatography (GPC), which was equipped with one 2414 RI detector and two separation columns (Waters, HT4 and HT5 columns), calibrated with PS standards. Mobile phase: THF (1.0 mL/ min at 35 °C). The polymer samples with a concentration of 2.0 mg/mL were tested in THF at 30 ℃ at a flow rate of 1.0 ml/min. Polystyrene standards were used for the calibration curve.

Differential Scanning Calorimetry (DSC). Crystallization temperature (T_c), melting temperature (T_m), and their enthalpies (ΔH_m)/(ΔH_c), glass transition temperature (T_g) related to thermodynamic properties of the samples were measured by differential scanning calorimetry (DSC) instrument using a TA Q20 instrument that was calibrated with indium. Measurements were performed under a nitrogen flow at a heating rate of 10 °C min^{-1} from -90 to 100 °C.

Wide-angle X-ray Diffraction (WAXD). All samples for WAXD were prepared by melting-compressed between two metallic disks. Then, they were quickly transferred to a heating treatment device with preset temperatures for 2 days. Dmax-Ultima þ X- ray diffract-tometer (Rigaku, Japan) with Ni-filtered Cu/K-α radiation (λ 1⁄4 0.15418 nm) are employed to detect the crystal structures at the scanning speed of 5° min^{-1} from 5° to 40° at 25°C. The operating target voltage was 40 kV, and the tube current was 100 mA.

MALDI-TOF MS. MALDI-TOF MS were performed on a MALDI MicroMX from Waters equipped with a 337 nm nitrogen laser. An accelerating voltage of 20 kV was applied. Mass spectra of 1000 shots were accumulated. The polymer sample was dissolved in CH_2Cl_2 at a concentration of 1 mg/mL. The cationization agent used was NaI dissolved in MeOH at a concentration 9-10 mg/mL. The matrix used was dithranol and was dissolved in CH_2Cl_2 at a concentration of 10 mg/mL. Solutions of matrix, salt, and polymer were mixed in a volume ratio of 3:1:1, respectively. The mixed solution was hand-spotted on a stainless steel MALDI target and left to dry. The spectrum was recorded in the reflection mode, and some with high molecular weight polymers are characterized by linear mode. Baseline corrections and data analyses were performed using MassLynx version 4.1 and Polymerix Software, Sierra Analytics, Version 2.0.0.

Polarized Optical Microscope. Leica DM4500P polarizing optical microscope with Linkam THMS600 hot stage was used to study the spherulitic morphology of the samples. The samples were completely melted in the hot stage and isothermally held at 100°C for 2 min. The sample was then cooled to the given temperature, and the growth of spherulitic morphology was monitored.

Equations and Calculations.

Compositional and conversional calculation of copolymers. HV and HP contents of P(HP-co-HV) copolymers were calculated according to the following equations (**ES1**)-(**SE2**) as ^1H NMR spectra in

Fig. 2 of P(3HP-co-5HV) copolymers with different compositions. The monomer conversions were calculated by the following equations (**ES3**)-(**ES5**) as *in-situ* ^{1}H NMR spectra in **Fig. S11**:

$$\mathrm{HVmol\%} = \frac{\mathrm{I_1}}{\mathrm{I_1+I_2}} \qquad \textbf{(ES1)}$$

$$\mathrm{HPmol\%} = \frac{\mathrm{I_2}}{\mathrm{I_1+I_2}} \qquad \textbf{(ES2)}$$

$$\mathrm{Con.\,VLmol\%} = \frac{\mathrm{I_1}}{\mathrm{I_1+I_3}} \qquad \textbf{(ES3)}$$

$$\mathrm{Con.\,MDOmol\%} = \frac{\mathrm{I_2}}{\mathrm{I_2+I_4+I_5}} \qquad \textbf{(ES4)}$$

$$\mathrm{Total\ conversion\ mol\%} = \frac{\mathrm{I_1+I_2}}{\mathrm{I_1+I_2+I_3+I_4+I_5}} \qquad \textbf{(ES5)}$$

where I_1 represents the integral at 4.05 ppm (two acetylenic protons of HV unit), I_2 represents the integration at 4.32 ppm (two protons of HP unit) in **Fig. 2** of P(3HP-co-5HV) copolymers with different compositions. I_3 represents the integral at 3.97 ppm (two acetylenic proton of δ-VL), I_4 and I_5 represent the integral at 3.55~3.65 ppm and 3.76~3.86 ppm (two protons of MDO) as *in-situ* ^{1}H NMR spectra in **Fig. S8**.

Nontermination model (**ES6**)- (**ES7**):

$$\mathrm{p_{MDOVL}(p_{MDO}) = 1 - n_{MDO}(1 - p_{MDO}) - (1 - n_{MDO})(1 - p_{MDO})^{r_{VL}}} \qquad \textbf{(ES6)}$$

$$\mathrm{p_{VLMDO}(p_{VL}) = 1 - n_{MDO}(1 - p_{VL})^{r_{MDO}} - (1 - n_{MDO})(1 - p_{VL})} \qquad \textbf{(ES7)}$$

where p_A=1−($A_{(t)}$/A_0) and p_B= are the respective monomer conversions of A and B, and p_{AB} is the total conversion of monomers.

Hoffman-weeks equation (ES8) for calculation of relative degree of the crystallinity **(ES9)**, and avrami equation **(ES10)** for calculation of the activation energy of the crystallization **(ES11)**:

$$\mathrm{T_m} = \mathrm{T_m^0}\left(1 - \frac{1}{\mathrm{r}}\right) \qquad \textbf{(ES8)}$$

$$X_\mathrm{t} = \frac{\int_0^\mathrm{t}\left(\frac{dH}{dt}\right)dt}{\int_0^{+\infty}\left(\frac{dH}{dt}\right)dt} \qquad \textbf{(ES9)}$$

$$X_{\mathrm{t}} = 1 - e^{(-k\mathrm{t}^{n})} \qquad \textbf{(ES10)}$$

$$K^{\frac{1}{\mathrm{n}}} = K_0 e^{-\frac{\Delta \mathrm{E}}{RT_{\mathrm{c}}s}} \qquad \textbf{(ES11)}$$

where **r** represents the thickening index, the higher thickening index means the larger layer thickness, X_{t} is the relative crystallinity, n is the avrami index, K_0 is the prefactor, and R is the universal gas constant, R = 8.314J·mol^{-1}·K^{-1}, T_{c} is the isothermal crystallization temperature.

Bragg equation (ES12) for the calculation of d-spacing:

$$2\mathrm{d}\sin\theta = \mathrm{n}\lambda \qquad \textbf{(ES12)}$$

where θ is the angle between X-rays and the corresponding crystal plane, λ is the wavelength of X-rays, n is the number of diffraction level.

The crystalline compatibility theories for the random copolymers. The crystallization theories for the random copolymers are generally divided into the following categories: the complete rejection theory (Flory equation **(ES13)**, Baur equation **(ES14)** etc.), the complete insertion theory (Sanchez-Eby equation **(ES15)**), and insertion-rejection theory (Wendling-Suter equation **(ES16-ES17)**), as follows:

Flory equation:

$$\frac{1}{T_m^0} - \frac{1}{T_{m(X_B)}} = \frac{R}{\Delta H_m^0}\ln(1 - X_B) \qquad \textbf{(ES13)}$$

Baur equation:

$$\frac{1}{T_m^0} - \frac{1}{T_{m(X_B)}} = \frac{R}{\Delta H_m^0}\ln(1 - X_B) - \langle 2X_B(1 - X_B\rangle^{-1} \textbf{ (ES14)}$$

Sanchez-Eby equation:

$$\frac{1}{T_m^0} - \frac{1}{T_{m(X_B)}} = \frac{R}{\Delta H_m^0}\ln(1 - X_B + X_{\mathrm{B}}e^{-\epsilon/RT}) \qquad \textbf{(ES15)}$$

Wendling-Suter:

$$\frac{1}{T_m^0} - \frac{1}{T_m(X_B)} = \frac{R}{R\Delta H_m^0}(\ln(1 - X_B + X_B e^{-\frac{\epsilon}{RT}}) - \langle\xi\rangle^{-1}) \textbf{ (E16)}$$

where

$$\langle\xi\rangle^{-1} = 2(X_B - X_B e^{-\epsilon/RT})(1 - X_B + X_B e^{-\epsilon/RT}) \quad \textbf{(E17)}$$

Synthesis and Characterization.

Synthesis of MDO. 2-Methyl-1,3-dioxan-4-one (MDO) was synthesized from racemic 2-methyl-dihydrofuran-3-one via Baeyer-Villiger oxidation. 85% m-CPBA (20g, 98 mmol, 2 eq.) was dissolved in 250 mL methylene chloride (DCM), dried over $MgSO_4$, and filtered. The filtrates were transferred into a 1000 mL dried three-necked flask equipped with mechanical stirring and spherical condenser under a nitrogen atmosphere and cooled to 0 °C. 2-Methyltetrahydrofuran-3-one (5 mL, 49 mmol, 1 eq.) was added stepwise via a syringe. The solution was then brought to room temperature and stirred for a further 4 h. The mixture was then washed with saturated sodium bicarbonate (8 × 20 mL) until no further carbon dioxide emission was evident. The aqueous fractions were extracted three times with DCM. The combined organic layers were washed with deionized water (10 mL) and subsequently dried over MgSO4. Dichloromethane was removed by distillation. The crude oil was transferred into a 25 mL round bottom flask, dried over calcium hydride for 3 h at room temperature and subsequently distilled via short path distillation apparatus (45 °C, 60Pa). The product was obtained as a colourless liquid (3.25g, 27.9 mmol, 65%) and stored at -23 °C in nitrogen. The purified product was characterised by 1H-, 13C-, COSY- and HSQC-NMR spectroscopy.

Synthesis of P3HP. A 10 mL flame-dried Schlenk tube with a Teflon stir bar was sealed prior to removal from the box. For a typical polymerization, racemic MDO monomer (generally 1g 10mmol) was added to a pressure vessel. Benzyl alcohol (BnOH) (0.2mL of a 0.025 M solution in toluene) was added as the initiator, Et_2Zn (0.2mL of a 0.05 M solution in toluene) was added as the catalyst. The mixture with an ultimate conversion of 80% for PHPA in 12h was stirred magnetically at room temperature. To quench

the polymerization, reaction vessels were opened to air, and the mixture was dissolved in DCM. Polymer was washed with methanol for several times, and then dried in a vacuum oven for 2 days.

Synthesis of P(3HP-co-5HV). The synthesis of 3HP-5HV 1:1 is described as an example. The polymerization of MDO (0.581g, 5mmol) and δ-VL (0.5 g, 5mmol) was performed as the synthetic route to P3HP. BnOH (0.2mL of a 0.025 M solution in toluene) as the initiator and Et_2Zn (0.2mL of a 0.05 M solution in toluene) as the catalyst were used. The polymerization time was at least 12 h. After quenching the polymerization, polymer was washed with methanol for several times, and then dried in a vacuum oven for 2 days.

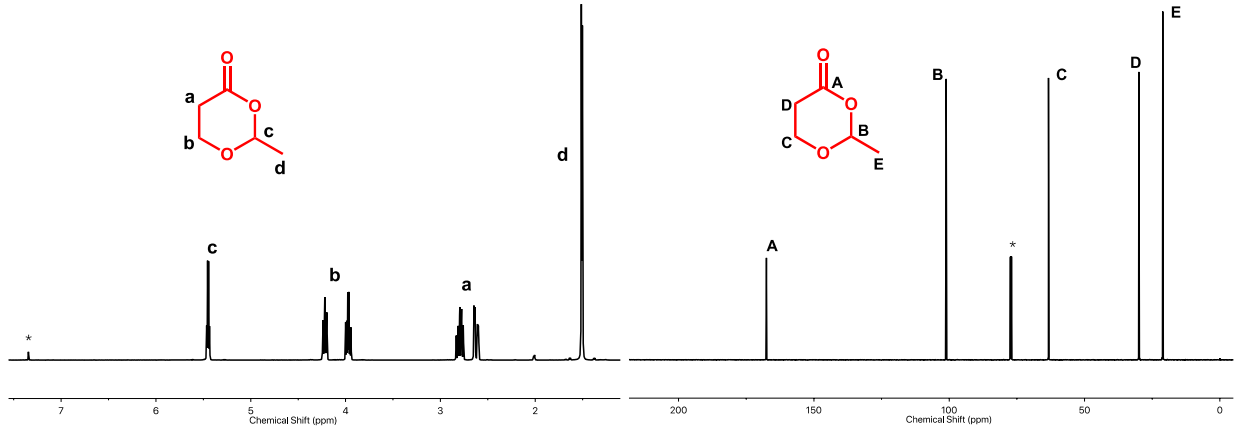

Fig. S1 ^{1}H-NMR and ^{13}C-NMR spectra of MDO

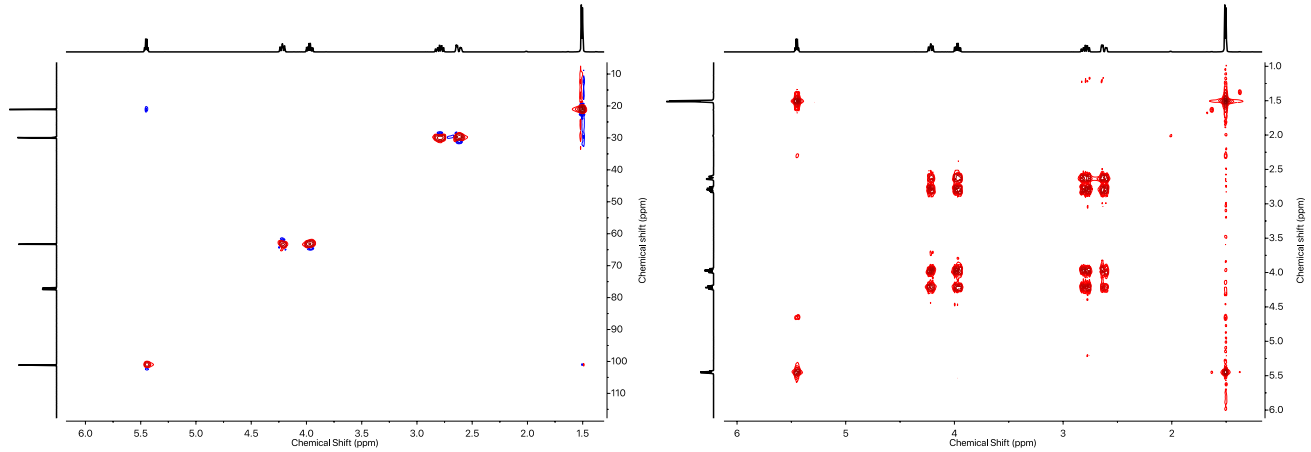

Fig. S2 ^{1}H-^{13}C COSY spectrum of MDO and ^{1}H-^{1}H HSQC spectrum of MDO

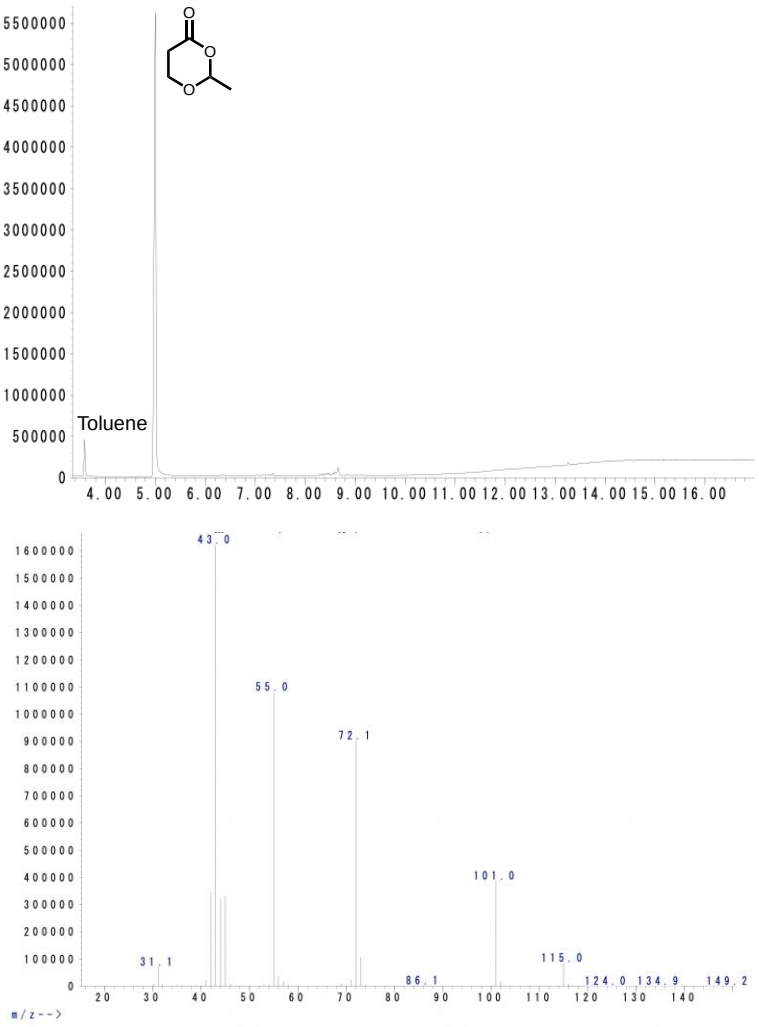

Fig. S3 GC-MS spectrum of purified MDO

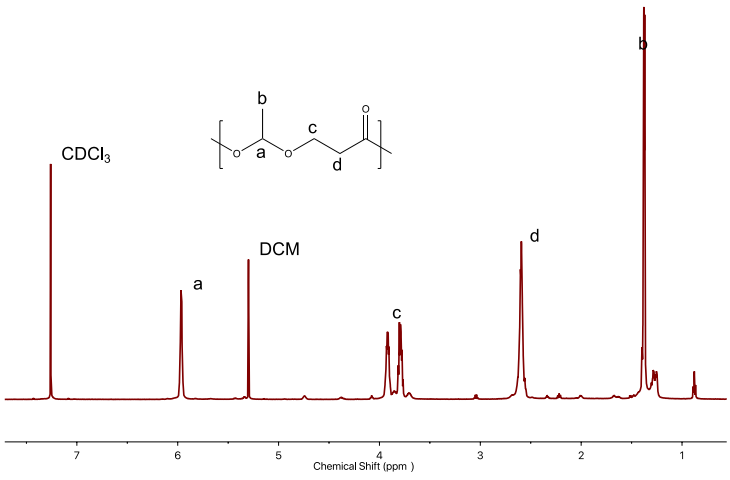

Fig. S4 ^{1}H-NMR spectrum of DPP catalyzed PMDO

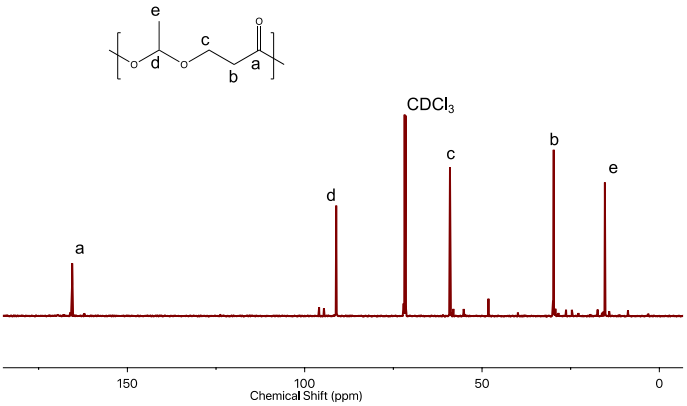

Fig. S5 ^{13}C-NMR spectrum of DPP catalyzed PMDO

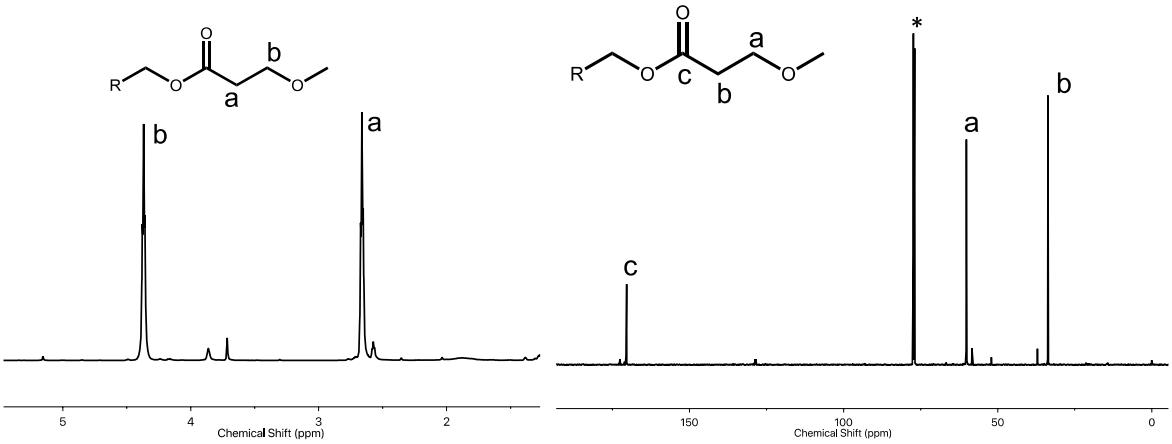

Fig. S6 ^{1}H-NMR and ^{13}C-NMR spectra of Et_2Zn catalyzed P3HP

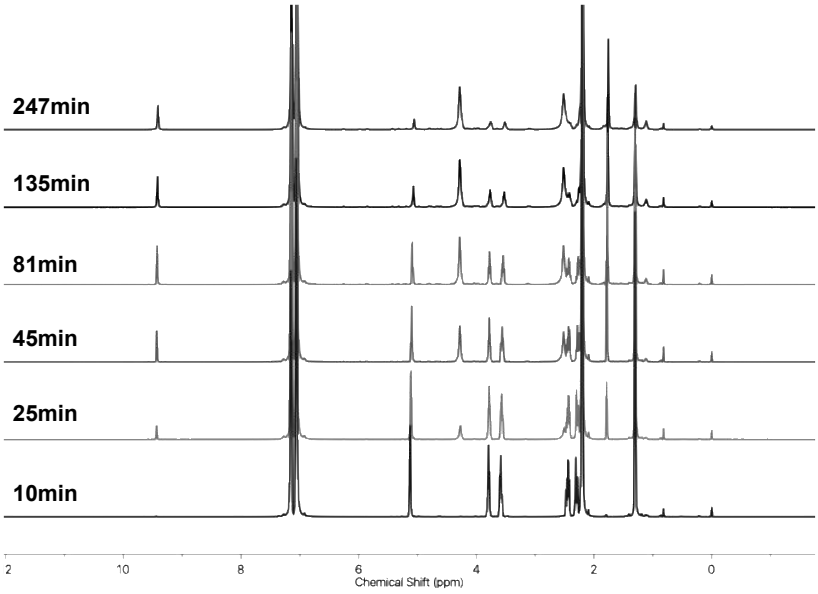

Fig. S7 The Et_2Zn catalyzed polymerization process of MDO monitored by *in-situ* ^{1}H-NMR spectra

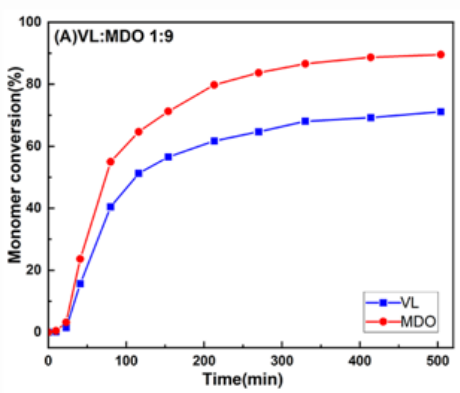
(A)VL:MDO 1:9
Monomer conversion(%)
Time(min)
VL
MDO

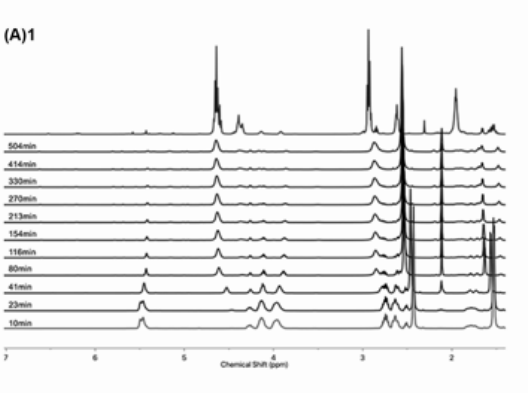
(A)1
504min
414min
330min
270min
213min
154min
116min
80min
41min
23min
10min
Chemical Shift (ppm)

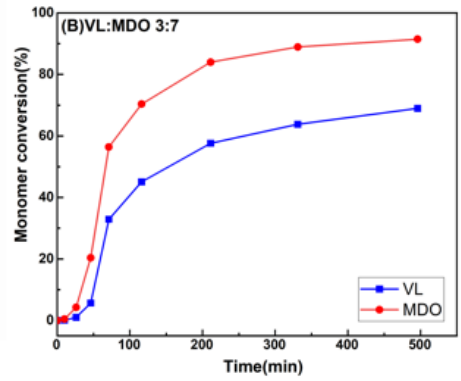
(B)VL:MDO 3:7
Monomer conversion(%)
Time(min)
VL
MDO

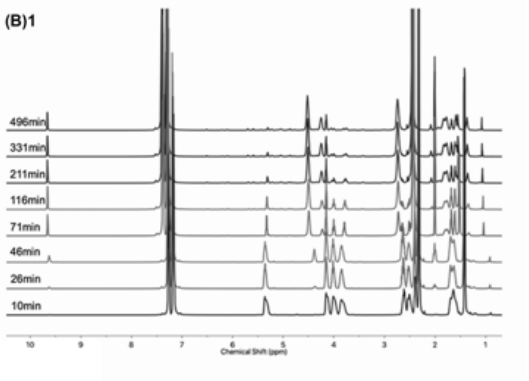
(B)1
496min
331min
211min
116min
71min
46min
26min
10min
Chemical Shift (ppm)

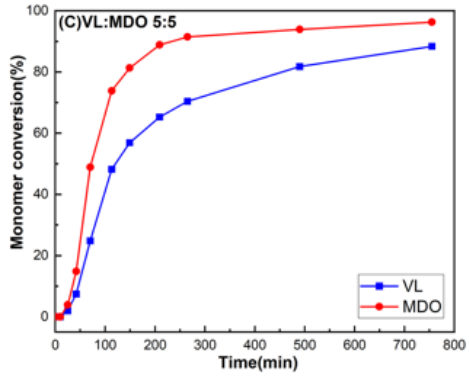
(C)VL:MDO 5:5
Monomer conversion(%)
Time(min)
VL
MDO

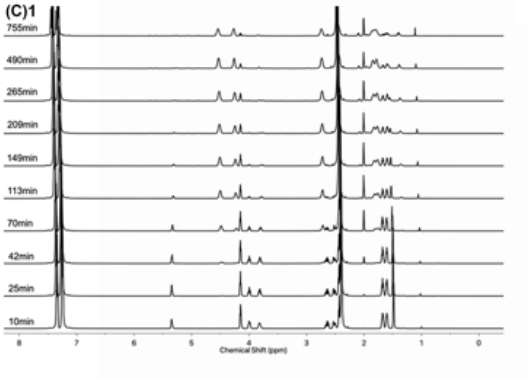
(C)1
755min
490min
265min
209min
149min
113min
70min
42min
25min
10min
Chemical Shift (ppm)

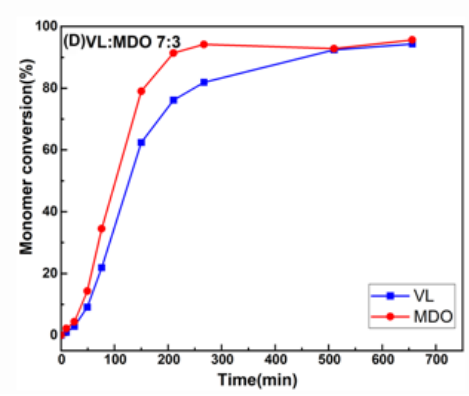
(D)VL:MDO 7:3
Monomer conversion(%)
Time(min)
VL
MDO

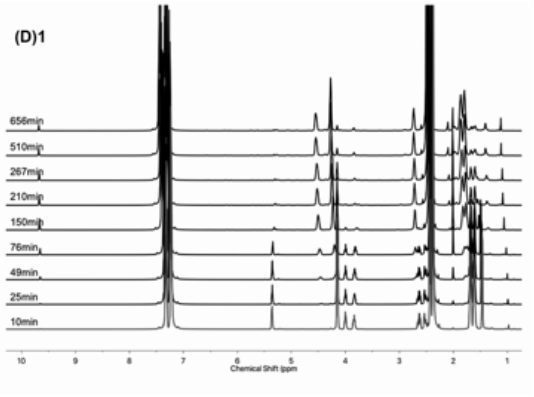
(D)1
656min
510min
267min
210min
150min
76min
49min
25min
10min
Chemical Shift (ppm)

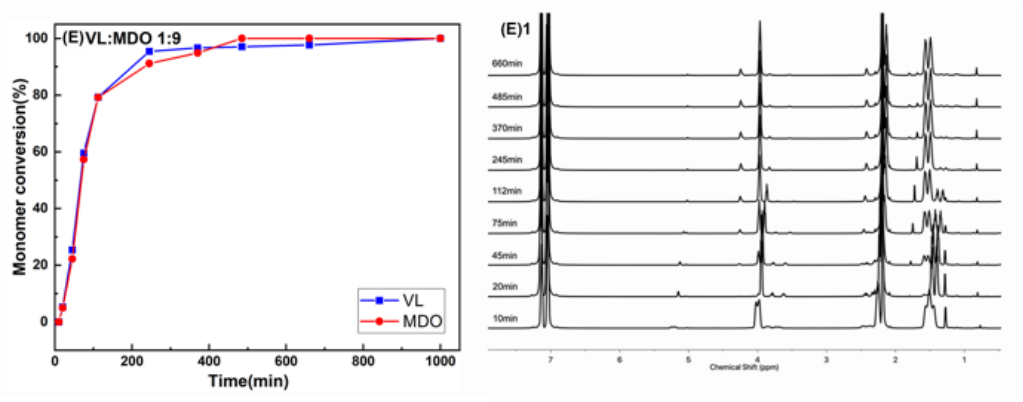

Fig. S8 Monomer conversion *vs* polymerization time curves evaluated from *in-situ* ^{1}H-NMR spectra of Et_2Zn catalyzed ROCOP of MDO and δ-VL during the polymerization process

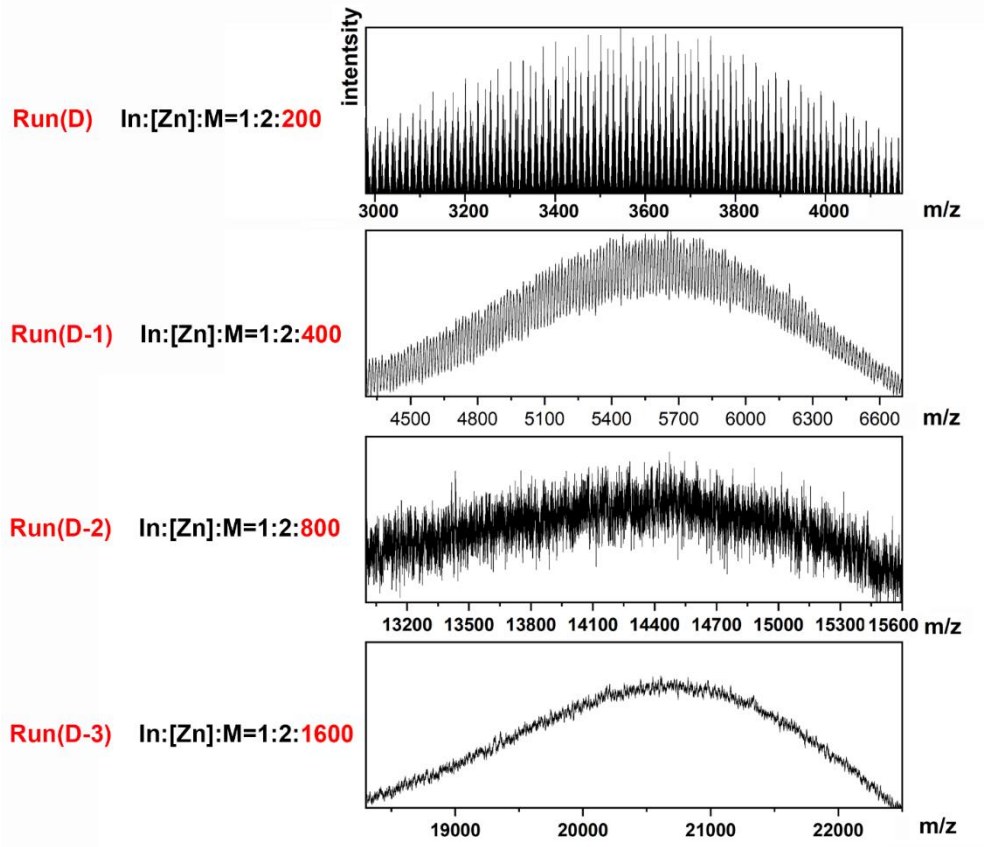

Fig. S9 MALDI-TOF MS of P(3HP-co-5HV), for In/[Zn]/M=1:2:200 (Run D), 1:2:400 (Run D-1), 1:2:800 (Run D-2), and 1:2:1600 (Run D-3) under the feed ratio of δ-VL:MDO=5:5. The images of the samples with the exact molecular weight (m/z＞5000) acquired in linear mode.

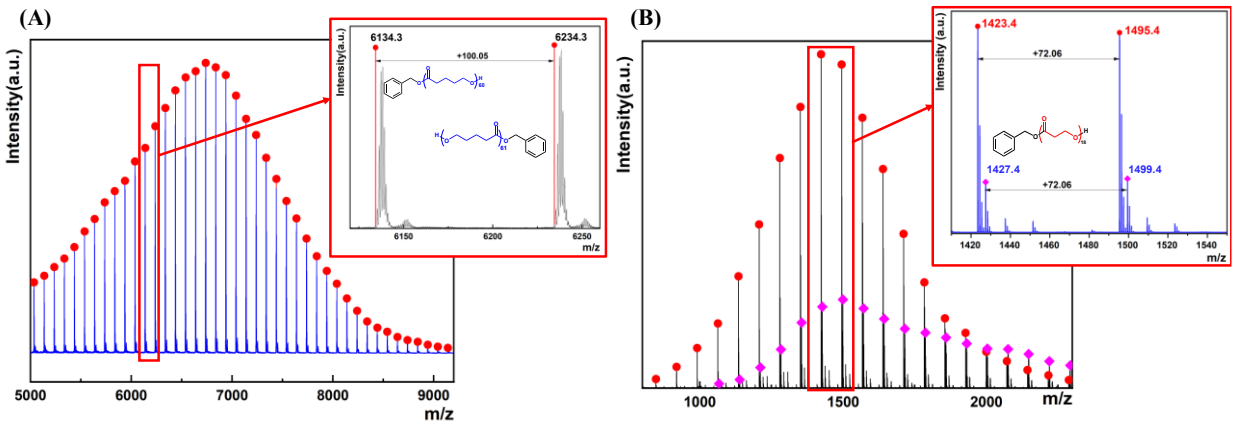

Fig. S10 MALDI-TOF MS of (A) P5HV and (B) P3HP

We have tried to make a further analysis of the possible chain transfer reaction. Firstly, a quick hypothesis is proposed that the end groups of the major peak series, i.e., m/z=1423.4/1495.4 (series 1) is ethane, which is possible from the initiation of the ethyl group of $ZnEt_2$.The product (series 2) initiated by BnOH is minor and the product (series 1) is major. While in P5HV (**Figure S10(B)**), only one set of peaks (series 2) appeared. As Hillmyer et al reported a proposed polymerization mechanism for the ROP of MDO, the aggregation of zinc propagating centers coordinated through alkoxide oxygens facilitates acetal elimination at higher relative catalyst concentrations. The two series of characteristic peaks with similar range of exact molecular weights for P3HP probably have a similar chain growth process for the ROP of MDO. However, the difference between the measured values of the series 1 and the theoretical values of ethane as the end group is 1.9, which is higher than 1. The hypothesis may not be appropriate for the ROP mechanism of MDO and requires further research. We elucidate the competitive relationship during the ROCOP process of MDO and δ-VL and the crystallization process of HP and HV. However, it is difficult for the P(3HP-co-5HV) copolymers to reveal the possible chain transfer reaction due to the complex MALDI-TOF MS.

Tab. S1. The exact molecular weight corresponding to MALDI-TOF MS as in **Fig. 5B**

VL:MDO 5:5	m/z (calc M+Na)	structure	observed	Δ	
1	3589.29	$HV_{18}HP_{23}$	3589.75	0.46	◆
2	3605.47	$HV_{16}HP_{26}$	3605.57	0.1	◇
3	3617.35	$HV_{19}HP_{22}$	3617.85	0.5	●
4	3621.56	$HV_{14}HP_{29}$	3621.39	-0.17	○
5	3633.53	$HV_{17}HP_{25}$	3633.67	0.14	★
6	3645.4	$HV_{20}HP_{21}$	3645.95	0.55	▼
7	3649.62	$HV_{15}HP_{28}$	3649.49	-0.13	▽
8	3661.49	$HV_{18}HP_{24}$	3661.77	0.28	◆
9	3677.29	$HV_{16}HP_{27}$	3674.05	0.3	◇
10	3689.54	$HV_{19}HP_{23}$	3689.87	0.33	●
11	3693.47	$HV_{14}HP_{30}$	3693.41	-0.06	○
12	3705.35	$HV_{17}HP_{26}$	3705.69	0.34	★
13	3717.32	$HV_{20}HP_{22}$	3717.97	0.65	▼
14	3721.44	$HV_{15}HP_{29}$	3721.51	0.07	▽
15	3733.41	$HV_{18}HP_{25}$	3733.79	0.38	◆
16	3745.28	$HV_{21}HP_{21}$	3746.07	0.79	☆
17	3749.88	$HV_{16}HP_{28}$	3749.61	-0.27	◇
18	3761.46	$HV_{19}HP_{24}$	3761.89	0.43	●
19	3774.39	$HV_{22}HP_{20}$	3774.17	-0.22	■
20	3777.26	$HV_{17}HP_{27}$	3777.71	0.45	★
21	3789.52	$HV_{20}HP_{23}$	3789.99	0.47	▼
22	3793.35	$HV_{15}HP_{30}$	3793.53	0.18	▽
23	3805.22	$HV_{18}HP_{26}$	3805.81	0.59	◆
24	3818.54	$HV_{21}HP_{22}$	3818.09	-0.45	☆
25	3821.03	$HV_{16}HP_{29}$	3821.63	0.6	◇
26	3833.28	$HV_{19}HP_{25}$	3833.91	0.63	●
27	3846.59	$HV_{22}HP_{21}$	3846.19	-0.4	■
28	3849.47	$HV_{17}HP_{28}$	3849.73	0.26	★
29	3861.34	$HV_{20}HP_{24}$	3862.01	0.67	▼
30	3865.17	$HV_{15}HP_{31}$	3865.55	0.38	▽
31	3877.43	$HV_{18}HP_{27}$	3877.83	0.4	◆
32	3890.45	$HV_{21}HP_{23}$	3890.11	-0.34	☆
33	3893.23	$HV_{16}HP_{30}$	3893.65	0.42	◇
34	3905.49	$HV_{19}HP_{26}$	3905.93	0.44	●
35	3918.51	$HV_{22}HP_{22}$	3918.21	-0.3	■
36	3921.67	$HV_{17}HP_{29}$	3921.75	0.08	★
37	3933.54	$HV_{20}HP_{25}$	3934.03	0.49	▼
38	3949.72	$HV_{18}HP_{28}$	3949.85	0.13	◆

39	3962.65	$HV_{21}HP_{24}$	3962.13	-0.52	☆
40	3965.43	$HV_{16}HP_{31}$	3965.67	0.24	◇
41	3978.45	$HV_{19}HP_{27}$	3977.72	-0.73	●
42	3990.33	$HV_{22}HP_{23}$	3990.23	-0.1	■
43	3993.49	$HV_{17}HP_{30}$	3993.77	0.28	★

Tab.S2 The exact molecular weight corresponding to MALDI-TOF MS as in **Fig. 5C**.

VL:MDO 5:5	m/z (calc M+Na)	structure	observed	Δ	
1	3702.91	$HV_{22}HP_{19}$	3702.15	-0.76	▲
2	3705.35	$HV_{17}HP_{26}$	3705.69	0.34	★
3	3717.32	$HV_{20}HP_{22}$	3717.97	0.65	▼
4	3721.44	$HV_{29}HP_{15}$	3721.51	0.07	▽
5	3730.79	$HV_{23}HP_{18}$	3730.13	0.66	■
6	3733.41	$HV_{18}HP_{25}$	3733.79	0.38	◆
7	3745.82	$HV_{21}HP_{21}$	3746.07	0.25	☆
8	3749.88	$HV_{16}HP_{28}$	3749.61	-0.27	◇
9	3758.91	$HV_{24}HP_{17}$	3758.35	-0.56	●
10	3761.46	$HV_{19}HP_{25}$	3761.89	0.43	●
11	3773.96	$HV_{22}HP_{20}$	3774.17	0.21	■
12	3777.26	$HV_{17}HP_{27}$	3777.71	0.45	★
13	3789.52	$HV_{20}HP_{23}$	3789.96	0.44	▼
14	3793.35	$HV_{15}HP_{30}$	3793.53	0.18	▽

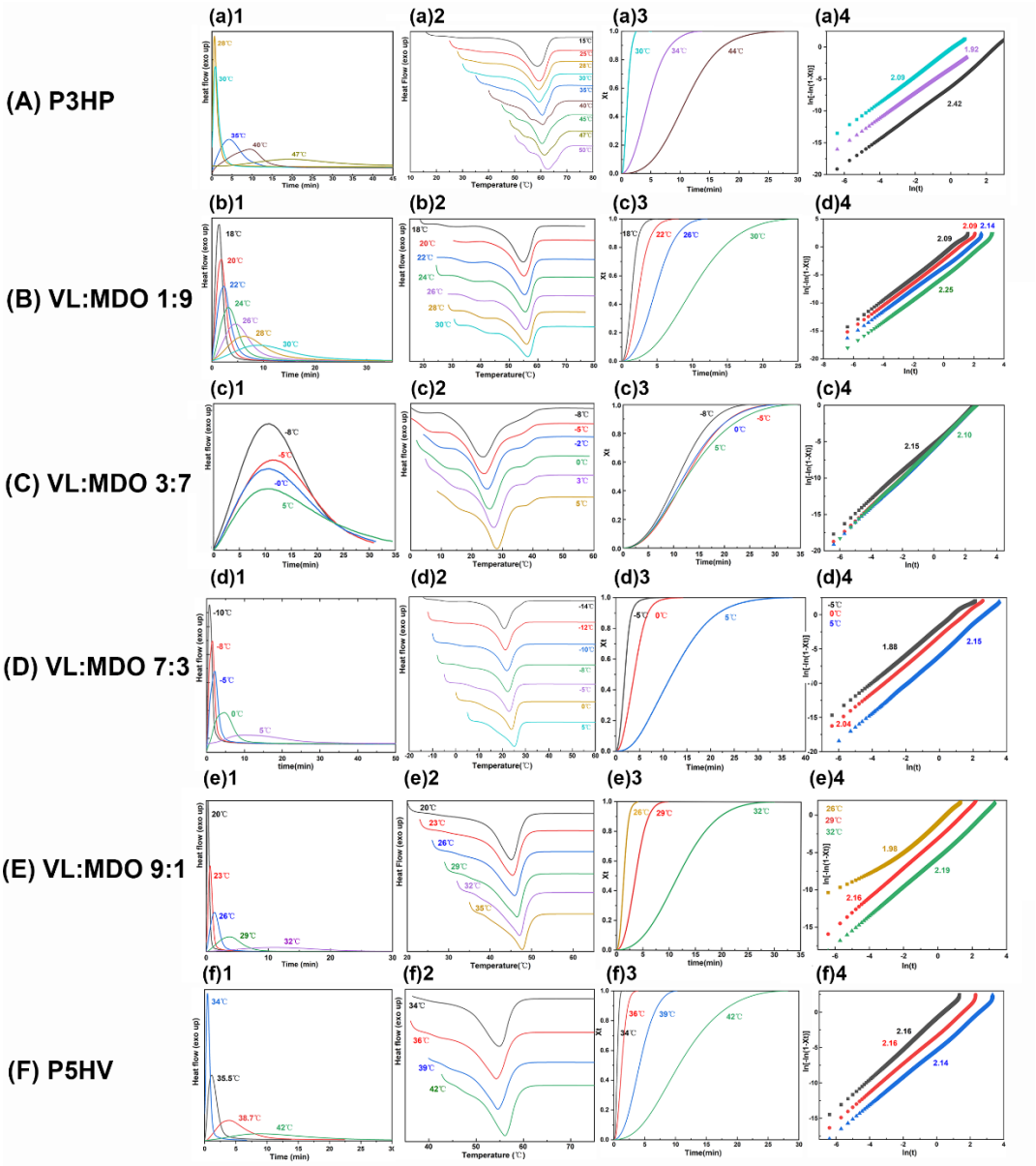

Fig. S11 The isothermal crystallization and melting behaviors determined by DSC of samples for (A) P3HP, (B) P(3HP-co-5HV) for feed ratio of δ-VL:MDO=1:9, (C) P(3HP-co-5HV) for feed ratio of δ-VL:MDO=3:7, (D) P(3HP-co-5HV) for feed ratio of δ-VL:MDO=7:3, (E) P(3HP-co-5HV) for feed ratio of δ-VL:MDO=9:1, (F) P5HV for (a1-d1) the isothermal crystallization heat flow-time curves at various temperatures of crystallization (T_cs) and (a2-f2) the subsequent melting traces, (a3-f3) the plots for the relative degree of crystallinity as a function of crystallization time at various T_cs, and (a4-f4) Avrami plots at various T_cs.

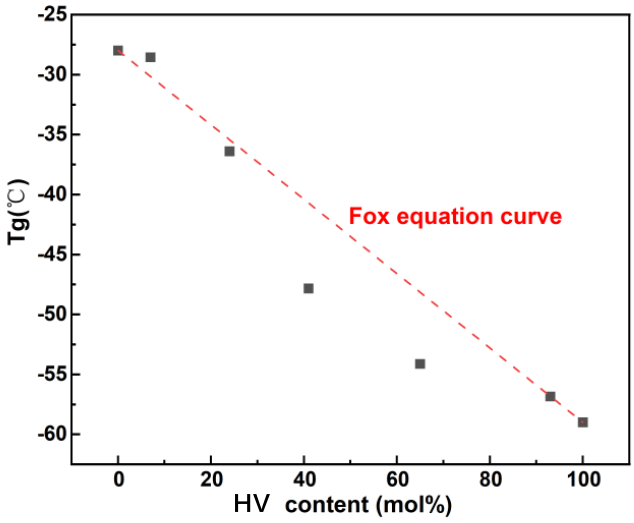

Fig. S12 The linear correlation curve for the dependence of T_g values on HV content

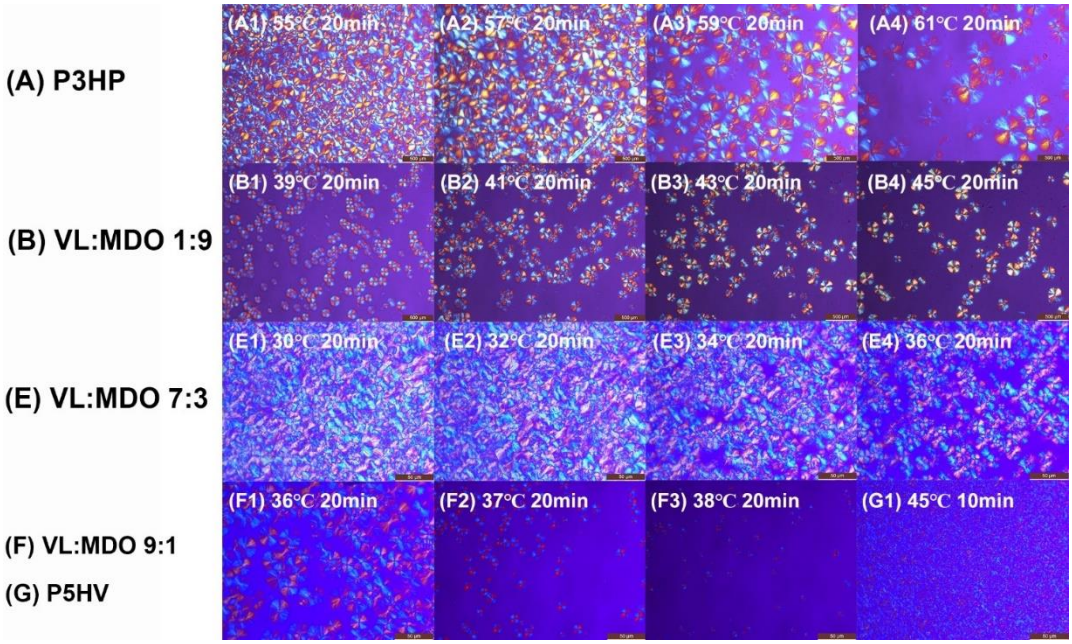

Fig. S13 POM micrograph (scale bar=50 μm) of (A) P3HP (A1-A4), (B) P(3HP-co-5HV) for feed ratio of δ-VL:MDO=1:9 (B1-B4), (E) P(3HP-co-5HV) for feed ratio of δ-VL:MDO=7:3 (E1-E4), (F) P(3HP-co-5HV) for feed ratio of δ-VL:MDO=9:1 (F1-F3), (G) P5HV G1 at different isothermal crystallization temperatures (T_cs).